



HAL
open science

Monitoring of phosphorylation using immobilized kinases by on-line enzyme bioreactors hyphenated with High-Resolution Mass Spectrometry

Justine Ferey, David da Silva, Cyril Colas, Pierre Lafite, Dimitrios Topalis, Vincent Roy, Luigi Agrofoglio, Richard Daniellou, Benoît Maunit

► To cite this version:

Justine Ferey, David da Silva, Cyril Colas, Pierre Lafite, Dimitrios Topalis, et al.. Monitoring of phosphorylation using immobilized kinases by on-line enzyme bioreactors hyphenated with High-Resolution Mass Spectrometry. *Talanta*, 2019, 205, pp.120120. 10.1016/j.talanta.2019.120120 . hal-03466045

HAL Id: hal-03466045

<https://hal.science/hal-03466045v1>

Submitted on 20 Dec 2021

HAL is a multi-disciplinary open access archive for the deposit and dissemination of scientific research documents, whether they are published or not. The documents may come from teaching and research institutions in France or abroad, or from public or private research centers.

L'archive ouverte pluridisciplinaire **HAL**, est destinée au dépôt et à la diffusion de documents scientifiques de niveau recherche, publiés ou non, émanant des établissements d'enseignement et de recherche français ou étrangers, des laboratoires publics ou privés.



Distributed under a Creative Commons Attribution - NonCommercial 4.0 International License

1 **Monitoring of phosphorylation using immobilized kinases by on-line enzyme bioreactors**
2 **hyphenated with High-Resolution Mass Spectrometry**

3 Justine Ferey^{1*}, David Da Silva¹, Cyril Colas^{1,2}, Pierre Lafite¹, Dimitrios Topalis³, Vincent
4 Roy¹, Luigi A. Agrofoglio¹, Richard Daniellou¹, Benoît Maunit¹

5 ¹ *Univ. Orléans, CNRS, ICOA, UMR 7311, F-45067 Orléans, France.*

6 ² *CNRS, CBM, UPR 4301, Univ-Orléans, F-45071, Orléans, France*

7 ³ *Rega Institute for Medical Research, KU Leuven, Herestraat 49 – box 1043, 3000, Leuven, Belgium*

8
9 • To whom correspondence should be addressed: Dr. Justine FERÉY,
10 justine.ferey@insa-rouen.fr

11 **Address:** Institut de Chimie Organique et Analytique (ICOA)

12 UMR-CNRS 7311

13 Université d'Orléans

14 Rue de Chartres

15 45067 Orléans cedex 02 – France

16

17 **E-mail address:** justine.ferey@insa-rouen.fr

18 **Tel:** +33 238492411

19 **Fax:** +33 238417281

20

21 **Abstract**

22 Nucleosides analogues are the cornerstone of the treatment of several human diseases. They
23 are especially at the forefront of antiviral therapy. Their therapeutic efficiency depends on
24 their capacity to be converted to the active nucleoside triphosphate form through successive
25 phosphorylation steps catalyzed by nucleoside/nucleotide kinases. In this context, it is
26 mandatory to develop a rapid, reliable and sensitive enzyme activity test to evaluate their
27 metabolic pathways. In this study, we report a proof of concept to directly monitor on-line
28 nucleotide multiple phosphorylation. The methodology was developed by on-line enzyme
29 bioreactors hyphenated with High-Resolution Mass Spectrometry detection. Human
30 Thymidylate Kinase (hTMPK) and human Nucleoside Diphosphate Kinase (hNDPK) were
31 covalently immobilized on functionalized silica beads, and packed into micro-bioreactors (40

32 μL). By continuous infusion of substrate into the bioreactors, the conversion of thymidine
33 monophosphate (dTMP) into its di- (dTDP) and tri-phosphorylated (dTTP) forms was
34 visualized by monitoring their Extracted Ion Chromatogram (EIC) of their $[\text{M-H}]^-$ ions. Both
35 bioreactors were found to be robust and durable over 60 days (storage at 4°C in ammonium
36 acetate buffer), after 20 uses and more than 750 minutes of reaction, making them suitable for
37 routine analysis. Each on-line conversion step was shown rapid (< 5 min), efficient
38 (conversion efficiency $> 55\%$), precise and repeatable ($\text{CV} < 3\%$ for run-to-run analysis).
39 The feasibility of the on-line multi-step conversion from dTMP to dTTP was also proved. In
40 the context of selective antiviral therapy, this proof of concept was then applied to the
41 monitoring of specificity of conversion of two synthesized Acyclic Nucleosides Phosphonates
42 (ANPs), regarding human Thymidylate Kinase (hTMPK) and *vaccina virus* Thymidylate
43 Kinase (vTMPK).

44

45 **Keywords:** Drug discovery, high resolution mass spectrometry, immobilized kinases, on-line
46 enzymatic phosphorylation.

47 **1. Introduction**

48 Drug discovery is a lengthy process. To gain a better understanding of the activity and
49 toxicity of pharmaceutical drugs, it is important to determine their metabolic pathways [1, 2].
50 The monitoring of conversion efficiency helps to optimize the drug development process. One
51 illustration of this latter is the activation of nucleotide analogues into their triphosphate active
52 form [3-5]. These compounds are the cornerstone of the treatment of several human diseases
53 and are especially at the forefront of antiviral therapy [6-9]. Biological activities are exhibited
54 by triphosphate nucleotides, which compete with natural substrates for incorporation in the
55 newly synthesized DNA strand, thus causing the inhibition of viral polymerase activity (e.g.

56 DNA chain termination) and therefore virus replication [10, 11]. To ensure good stability and
57 high availability, these compounds are delivered as uncharged molecules [12]. Two major
58 antiviral nucleoside classes have proved to be biologically active: the nucleoside analogues
59 [13] and the Acyclic Nucleoside Phosphonate (ANPs) analogues [7]. Since the rate-limiting
60 step of the drug activation is the conversion of nucleoside analogues to their monophosphate
61 form, nucleotide analogues as ANPs were designed to circumvent the initial phosphorylation
62 activation step [14]. The phosphorylation process of a monophosphate to its triphosphate
63 counterpart involves two successive enzymatic phosphorylation reactions catalyzed by
64 cellular kinases [14, 15]. For instance, the conversion of the endogenous thymidine
65 monophosphate (dTMP) to thymidine triphosphate (dTTP) is catalyzed by the human
66 Thymidylate Kinase (hTMPK) and the human Nucleoside Diphosphate Kinase (hNDPK)
67 [11]. This activation is performed by a phosphotransfer reaction from a donor, usually the γ -
68 phosphate of adenosine-5'-triphosphate (ATP), towards an acceptor such as the 5'-OH
69 nucleoside or α -, β -phosphate nucleotide groups, in the presence of a chelating agent (usually
70 Mg^{2+}) [3-5, 16]. To the best of our knowledge, the main techniques used to determine the
71 efficiency of a kinase catalyzed reaction are spectrophotometric [17-19], radioisotopic [20-
72 22], High Performance Liquid Chromatography (HPLC) [23] and Capillary Electrophoresis
73 (CE) [24-26]. Although all these techniques have shown their potential for the study of kinase
74 activity, the development of an on-line mass spectrometric approach makes sense in view of
75 its rapidity, substrate versatility and specificity of detection. These on-line methodologies are
76 currently gaining interest for application in drug discovery [27-32]. This liquid
77 chromatography methodology uses biological agents as stationary phase to study
78 enzyme/ligand interactions [33]. Enzyme-immobilized bioreactors offer usually various
79 advantages such as purification of the biological environment (low matrix effect),
80 preservation of activity, bioreactor stability (possible reuse), ease of analysis, easy coupling

81 with the detection system, direct conversion monitoring and possible high throughput
82 screening of compound mixtures. Recently, the use of on-line methodologies with a single
83 bioreactor or multi-reactor have been presented in the field of substrate conversion monitoring
84 [34, 35] or DNA digestion [36].

85 In this context, the present study aimed to develop a rapid, efficient and versatile on-line
86 methodology for the direct monitoring of nucleoside monophosphate and nucleotide
87 diphosphate phosphorylation. As a proof of concept, individual conversion of dTMP into
88 dTDP and dTDP into dTTP were monitored by on-line infusion into immobilized hTMPK
89 and hNDPK bioreactors. The feasibility of the on-line two successive phosphorylation steps
90 was also evaluated. This on-line system showed various advantages such as a rapid (less than
91 5 minutes) and efficient (more than 50%) conversion. Moreover, thanks to the dual loop
92 system, this system is versatile (successive substrate infusion) and automatable. It also allows
93 to directly visualize the drug conversion with the specific detection by mass spectrometry.
94 This developed on-line methodology was then applied to the qualitative study of specificity of
95 conversion of two chemically synthesized Acyclic Nucleotides Phosphonates (ANPs) named
96 ANP-CH₃ and ANP-Br [37] (molecular formula shown in Figure 1) regarding two TMPKs:
97 *vaccina virus* TMPK (vvTMPK) and human TMPK (hTMPK).

98 **2. Experimental section**

99 **2.1. Material**

100 Thymidine 5'-monophosphate disodium salt hydrate (dTMP), thymidine 5'-diphosphate
101 sodium salt (dTDP), thymidine 5'-triphosphate sodium salt (dTTP), adenosine 5'-triphosphate
102 magnesium salt (ATP), ammonium acetate (AcNH₄) and magnesium chloride (MgCl₂) were
103 purchased from Sigma-Aldrich (Saint-Quentin-Fallavier, France). For each experiment,
104 AcNH₄ was used at 50 mM ionic strength at pH = 7. The bioreactor (50 x 1 mm stainless steel

105 capillary), column end fitting, high pressure unions, back pressure regulator (500 psi) and
106 PEEK tubing (1 mm and 0.75 mm) were purchased from Cluzeau Info Labo (Sainte-Foy-La-
107 Grande, France). The de-ionized water used in all procedures was purified with an Elgastat
108 UHQ II system (Elga, Antony, France). Plasmids bearing hTMPK, *v*vTMPK and recombinant
109 hNDPK were a generous gift from the University Pierre et Marie Curie (UPMC-Paris 6).
110 Recombinant hTMPK was produced and purified as previously described [38]. Acyclic
111 nucleoside monophosphates ANP-CH₃-MP and ANP-Br-MP were synthesized as described in
112 our previous work [37].

113 2.2. Instrumentation

114 Experiments were performed on a Bruker maXis UHR-Q-TOF spectrometer (Bremen,
115 Germany) in negative ion mode. The mass spectrometer was coupled on-line with a Dionex
116 UltiMate 3000 RSLC system (Germering, Germany). Before each experiment, calibration was
117 performed using ES-TOF tuning mix (Agilent Technologies, Les Ulis, France). The capillary
118 voltage was set at - 4000 V, the nebulizer pressure at 0.6 bar, the dry gas flow at 7.0 L min⁻¹
119 and heated at 200°C. Spectra were recorded within the mass range from *m/z* 50 to 1350.
120 Chromatograms of the ions of interest (*m/z* 321.0500 [M-H]⁻ for dTMP, *m/z* 401.0166 [M-H]⁻
121 for dTDP and *m/z* 480.9831 [M-H]⁻ for dTTP, *m/z* 259.0562 [M-H]⁻ for ANP-CH₃-MP, *m/z*
122 322.0561 [M-H]⁻ for ANP-Br-MP, *m/z* 339.0150 [M-H]⁻ for ANP-CH₃-DP and *m/z* 402.0149
123 [M-H]⁻ for ANP-Br-DP) were generated as Extracted Ion Chromatograms (EIC) within a ±
124 0.005 *m/z* range. *m/z* values are summarized in Table 1. All data were analyzed using
125 DataAnalysis 4.4 software (Bruker).

126 2.3. Enzyme immobilization

127 hTMPK, *v*vTMPK and hNDPK immobilizations were performed following a previous study
128 [39]. Briefly, separate immobilizations *via* glutaraldehyde cross-linking agent were performed

129 by placing the enzyme in contact with 30 mg of silica beads diluted in phosphate buffer (500
130 μL , 50 mM ionic strength, $\text{pH} = 7$) with final excess concentrations of 0.55 mg mL^{-1} of
131 hTMPK and $\nu\nu\text{TMPK}$ and 1.8 mg mL^{-1} of hNDPK. The three solutions were stirred for 6 h at
132 4°C and then stored overnight with 1 mM glycine at 4°C . Remaining free hTMPK, $\nu\nu\text{TMPK}$
133 and hNDPK were removed by successive washings (AcNH_4).

134 **2.4. Bioreactor packing**

135 Each immobilized enzyme solution was placed in a tank (100 x 4.6 mm) connected to the
136 bioreactor (50 x 1 mm) by means of a PEEK tube of 1 mm id and a true zero dead volume
137 union. A frit was placed at the end of the bioreactor to retain the silica beads. AcNH_4 buffer
138 was eluted through the tank with a semi-micro HPLC pump (PU-2085 Plus, Jasco, Tokyo,
139 Japan). Start flow was set at $10 \mu\text{L min}^{-1}$ and was gradually increased to reach a maximum
140 pressure of 30 bar. After 1 h of elution, a back-pressure regulator was added at the end of the
141 bioreactor. At the maximum pressure of 40 bar, silica was considered packed into the
142 bioreactors. The bioreactor denaturation was performed by overnight MeOH infusion at 60
143 $\mu\text{L min}^{-1}$.

144 **2.5. On-line fluidic system**

145 As shown in Figure 2, the on-line system consisted in a high flow rate precision pump and a
146 ten-port valve containing 2 injection loops connected to the bioreactors (active and
147 denatured). AcNH_4 buffer was eluted at $40 \mu\text{L min}^{-1}$ (or $60 \mu\text{L min}^{-1}$) through the ten-port
148 valve. On this valve, two $320 \mu\text{L}$ injection loops, build with 0.75 mm id PEEK tubes were
149 placed in back flush configuration (Figure S1). Injections were made at position 7 by means
150 of an autosampler. The autosampler injected $400 \mu\text{L}$ of a solution “1” into the loop 1 (position
151 valve 1-2) with the loading pump. The valve then switches to position 1-10 to infuse solution
152 “1” into the bioreactors with the analytical pump (AcNH_4 buffer). During loop 2 infusion, the

153 loop 1 is washed with AcNH₄ buffer and a solution “2” is loaded into the loop 2 with the
154 loading pump (position valve 1-10). When the infusion is completed, the valve switches to
155 position 1-2 and loop 2 is infused. Solutions “1” and “2” can be the same for a longer time
156 infusion or can be different for a screening approach. Each parameter (time infusion,
157 injection, valve position) is programmed manually in the method (script editor). The valve
158 switched every 3 or 5 minutes (for flow rates of 60 $\mu\text{L min}^{-1}$ and 40 $\mu\text{L min}^{-1}$, respectively).
159 The two bioreactors, joined in series at 37°C in an oven, are connected to the ten-port valve at
160 position 4 from the inlet and directly linked to the electrospray source from the outlet.

161 **2.6. Validation of the on-line methodology for individual or multi-step enzymatic** 162 **reaction**

163 **2.6.1. hTMPK bioreactor conversion**

164 The bioreactor was conditioned at 37°C by AcNH₄ buffer elution for 15 minutes at a flow rate
165 of 60 $\mu\text{L min}^{-1}$. 400 μL of a 20 μM dTMP solution (AcNH₄, [ATP] = 150 μM , [MgCl₂] = 200
166 μM ,) were injected *via* the loop system as previously described. After the valve switch, the
167 sample contained in the loop was eluted with AcNH₄ at a flow rate of 60 $\mu\text{L min}^{-1}$ (P = 10
168 bar) into the hTMPK bioreactor. During the first loop infusion, 400 μL of the same dTMP
169 solution were injected into the second loop. After 3 minutes of infusion, the valve was
170 switched to infuse the second loop. This process was repeated until the EIC plateau for dTMP
171 and dTDP was reached. The bioreactor was then washed and the enzymes were regenerated
172 with AcNH₄ at 100 $\mu\text{L min}^{-1}$ until elimination of the substrate and product from the capillary.
173 Between each use, the hTMPK bioreactor was stored at 4°C in AcNH₄. The same
174 methodology was applied to the vvTMPK bioreactor study.

175 **2.6.2. hNDPK bioreactor conversion**

176 The hNDPK bioreactor was conditioned as previously described. The dTDP solution (20 μM
177 in AcNH_4 , $[\text{ATP}] = 150 \mu\text{M}$, $[\text{MgCl}_2] = 200 \mu\text{M}$) was continuously infused into the hNDPK
178 bioreactor at a flow rate of $40 \mu\text{L min}^{-1}$ (5 minutes between each valve switch). Analyses
179 were performed after dTDP and dTTP EIC plateau monitoring. The bioreactor was then
180 washed and the enzymes were regenerated with AcNH_4 at $100 \mu\text{L min}^{-1}$ until elimination of
181 the substrate and product. Between each use, the hNDPK bioreactor was stored at 4°C in
182 AcNH_4 .

183 **2.6.3. Multi-step phosphorylation with hTMPK and hNDPK bioreactors in** 184 **series**

185 The bioreactors were placed in series *via* a stainless steel high-pressure union. 20 μM dTMP
186 solution ($[\text{ATP}] = 150 \mu\text{M}$, $[\text{MgCl}_2] = 200 \mu\text{M}$) was infused at $40 \mu\text{L min}^{-1}$ ($P = 11 \text{ bar}$) as
187 previously described (5 minutes between each valve switch). Analysis was stopped after
188 monitoring the dTMP, dTDP and dTTP EIC plateaus. The bioreactors were washed and the
189 enzymes were regenerated with AcNH_4 elution at $80 \mu\text{L min}^{-1}$.

190 **2.6.4. Stability and reuse of the hTMPK and hNDPK bioreactors study**

191 *hTMPK bioreactor:* 20 μM dTMP solution ($[\text{ATP}] = 150 \mu\text{M}$, $[\text{MgCl}_2] = 200 \mu\text{M}$) was
192 infused at $60 \mu\text{L min}^{-1}$ with AcNH_4 in the hTMPK bioreactor. Seven points of activity were
193 recorded over 60 days. Over this period, the bioreactor was used 21 times, corresponding to
194 795 min of use. The hTMPK bioreactor was alternatively used and stored at 4°C in AcNH_4
195 for 60 days.

196 *hNDPK bioreactor:* 20 μM dTDP solution ($[\text{ATP}] = 150 \mu\text{M}$, $[\text{MgCl}_2] = 200 \mu\text{M}$) was
197 infused at $40 \mu\text{L min}^{-1}$ with AcNH_4 in the hNDPK bioreactor. Seven points of activity were
198 recorded over 68 days (20 uses, corresponding time of use 915 minutes). The hNDPK
199 bioreactor was alternatively used and stored in ammonium acetate buffer at 4°C for 68 days.

200 **2.7. Application of the on-line methodology for the study of two ANPs specific**
201 **conversion regarding hTMPK and $\nu\nu$ TMPK**

202 hTMPK and $\nu\nu$ TMPK bioreactors were individually placed in the fluidic system as described
203 **in paragraph 2.6.1.** The bioreactors were conditioned at 37°C with AcNH₄ buffer elution for
204 15 min at a flow rate of 60 $\mu\text{L min}^{-1}$. 400 μL of 20 μM of each substrate solution (dTMP,
205 ANP-CH₃-MP and ANP-Br-MP in AcNH₄, [ATP] = 150 μM and [MgCl₂] = 200 μM ,) were
206 injected via the loop system as previously described. Substrate solutions were continuously
207 infused until the detection of EIC plateau. Between each substrate infusion, the bioreactors
208 were washed and the enzymes were regenerated with AcNH₄ at 100 $\mu\text{L min}^{-1}$ until
209 elimination of substrate and product from the capillary.

210 **3. Results and discussion**

211 **3.1. Monitoring phosphorylation – Optimization of the on-line methodology**
212 **conditions**

213 In this study, optimizations of the system were conducted. The phosphodonor and chelatan
214 concentrations were evaluated for the conversion efficiency and the fluidic system and the
215 bioreactor packing (Figure S2) were optimized. The influence of [ATP] and [MgCl₂] on
216 ionization and on the mono-phosphorylation step was evaluated in our previous study with the
217 same enzymes [39]. The optimal concentration of the phosphodonor (ATP) for on-line
218 conversion was evaluated for the first reaction step, using the hTMPK bioreactor. Based on
219 the results shown in Figure S3, the optimum concentration was fixed at 150 μM of ATP, in
220 terms of conversion rate, conversion speed and detector saturation. This concentration was
221 then fixed for the study of the hNDPK bioreactor.

222 The immobilization step was carried out with high enzymes concentrations in order to saturate
223 the immobilization sites as described in our previous study [39]. Free and immobilized

224 enzyme activities were evaluated by FIA-HRMS. The immobilized enzyme activities were
225 evaluated by Michaelis-Menten study by Flow Injection Analysis hyphenated with High
226 Resolution Mass Spectrometry, as described in our last work [39]. Briefly, similar K_M values
227 for immobilized and free enzymes were obtained regarding dTMP [$K_{M(\text{free hTMPK})} = 34.43 \pm$
228 $5.05 \mu\text{M}$, $K_{M(\text{immobilized hTMPK})} = 27.92 \pm 4.14 \mu\text{M}$ and $K_{M(\text{free hNDPK})} = 92.75 \pm 12.80 \mu\text{M}$,
229 $K_{M(\text{immobilized hNDPK})} = 132.90 \pm 18.50 \mu\text{M}$], showing that the immobilization step does not
230 influence the enzyme's affinity towards its substrate. The reaction speed (V_{max}) of the
231 immobilized enzymes was reduced by half [$V_{\text{max}(\text{free hTMPK})} = 6.86 \pm 0.51 \mu\text{M min}^{-1}$,
232 $V_{\text{max}(\text{immobilized hTMPK})} = 2.94 \pm 0.17 \mu\text{M min}^{-1}$ and $V_{\text{max}(\text{free hNDPK})} = 13.01 \pm 1.27 \mu\text{M min}^{-1}$,
233 $V_{\text{max}(\text{immobilized hNDPK})} = 6.41 \pm 0.36 \mu\text{M min}^{-1}$]. Immobilized hTMPK and hNDPK activities
234 were proved to be sufficient to evaluate on-line phosphorylation reactions. In this context,
235 these enzymes were used for the on-line reactions studies.

236 As shown in Figure 2, the system consists of a dual injection loop (2 loops of 320 μL)
237 connected to a ten-port valve. The volume of the two loops, arbitrarily fixed at 320 μL to
238 obtain an elution time of 5 min for each one (flow rate fixed at 50 $\mu\text{L min}^{-1}$), is adjustable
239 depending on the elution time required. This system provides a constant ligand infusion into
240 the bioreactors with high versatility (no mobile phase changes or lengthy reconditioning
241 between ligand analyses) and without LC system salt contamination. Ligand injection into the
242 loop can be performed manually by means of a syringe (for method development) or by
243 programming automatic injection *via* the use of a second pump and an autosampler. This
244 automation makes the system compatible for routine analysis and for molecule screening.
245 Each bioreactor was evaluated for one-step reaction in terms of feasibility, conversion rates,
246 stability and analysis repeatability. For both bioreactors, each specific substrate (dTMP and
247 dTDP) was infused into active and denatured hTMPK and hNDPK bioreactors respectively, to
248 estimate false positive conversion detection and to evaluate non-specific interactions. The

249 feasibility of the on-line two successive phosphorylations was then evaluated before the
250 application study.

251 **3.2. Validation of the on-line approach for single step phosphorylation monitoring**

252 **3.2.1. hTMPK bioreactor**

253 The conversion of nucleoside monophosphate into nucleoside diphosphate is known to be the
254 reaction-limiting step [10, 14]. hTMPK bioreactor conversion was evaluated by natural
255 substrate (dTMP) infusion. The reaction was directly checked by monitoring the specific EIC
256 of the masses of interest. During the infusion step ($60 \mu\text{L min}^{-1}$) the substrate first bound to
257 the enzyme. After full saturation of the active sites, dTMP passed through the bioreactor and
258 the EIC related to the non-retained substrate appeared. The product was then released from
259 the bioreactor and the dTDP EIC was delayed. Figure 3 shows the EIC of dTMP and dTDP
260 during the infusion of dTMP solution into the denatured and active bioreactor. No conversion
261 was achieved with the denatured hTMPK bioreactor, attesting the lack of a false positive. In
262 the case of active hTMPK, dTDP appeared rapidly, after 2 min of infusion (30 s after dTMP
263 accumulation). The plateau conversion was quickly reached after 4 min of dTMP infusion.
264 Compared to the experiment with denatured enzyme, a decrease in dTMP intensity was
265 observed (from 3.8×10^5 a.u for denatured to 1.2×10^5 a.u for active hTMPK) and the plateau
266 was delayed (from 4 to 8 minutes), which confirmed the substrate consumption. The
267 remaining dTMP EIC intensity was not directly correlated to the non-conversion of dTMP
268 into dTDP but it was also due to in-source dTDP fragmentation. This fragmentation could be
269 estimated at 20% by analyzing a range of dTDP concentrations (5-50 μM). The on-line
270 conversion efficiency of dTMP into dTDP was therefore estimated at 67%. Although a
271 decrease in dTMP intensity can be noted (4.3 min, active hTMPK), the feasibility and the
272 non-interference of the switch loop system during valve rotation is proved. This experiment

273 attested both the feasibility of an on-line phosphorylation and the ability to ensure constant
274 substrate infusion *via* the use of the dual switch loop system developed for this study.

275 **3.2.2. hNDPK bioreactor**

276 To validate the versatility of this method, the hNDPK bioreactor activity was checked by
277 dTDP infusion. As shown in Figure 4, similar results were obtained. The absence of
278 conversion, using denatured hNDPK, attested the lack of false-positive whereas product
279 accumulation (dTTP) was observed with the active bioreactor. Total conversion of dTDP into
280 dTTP was observed. The remaining intensity of dTDP EIC is due to the estimated 50% of
281 dTTP fragmentation. The full conversion is due to the higher V_{\max} value of immobilized
282 hNDPK ($V_{\max(\text{immobilized hNDPK})} = 6.4 \mu\text{L min}^{-1}$ and $V_{\max(\text{immobilized hTMPK})} = 2.9 \mu\text{L min}^{-1}$) that enable
283 a faster conversion. This maximal velocity has an even more important influence on the
284 conversion rate in on-line enzymatic conversion. These experiments proved the feasibility to
285 efficiently (conversion estimation > 60%) and rapidly (< 5 minutes) monitor individual on-
286 line phosphorylation.

287 **3.3. Validation of the on-line approach for multi-step phosphorylation monitoring**

288 On-line individual reactions were shown to be feasible and efficient by the present
289 methodology. The feasibility of the direct monitoring of dTTP accumulation by the on-line
290 multi-step enzymatic reaction was studied, as a proof of concept, by placing the two
291 bioreactors in series in the LC system. The conversion of dTMP into its di- and tri-phosphate
292 form was directly monitored by EIC. Similar conditions to those previously described were
293 applied. Figure 5 shows the EIC of the masses of interest. The initial substrate (dTMP)
294 appeared after 5 min of infusion whereas the accumulation of the intermediate (dTDP) and
295 final products (dTTP) appeared at 10 minutes, reaching a plateau at around 25 minutes.
296 Conversion was shown to be efficient with 55% of dTMP converted into dTTP. The high

297 intensity of dTMP EIC is due to the limiting step of dTMP conversion into dTDP but also due
298 to the fragmentation of dTDP and dTTP as explained above. The cascade efficiency was
299 consistent with individual reaction efficiencies (55% conversion of dTMP into dTTP for the
300 cascade against 67% and 100 % for each individual bioreactor).

301 **3.4. Bioreactor repeatability and reuse study**

302 The system repeatability and stability were further evaluated. The repeatability of hTMPK
303 and hNDPK bioreactor activities was studied through three successive infusions (n = 3) of
304 dTMP (hTMPK bioreactor) and dTDP (hNDPK bioreactor). Relative standard deviations for
305 run-to-run analysis were acceptable with 2.42% for the hTMPK bioreactor and 2.36 % for the
306 hNDPK bioreactor. Longevity was investigated by monitoring bioreactor activities over
307 several days. Figure 6 shows a decrease in normalized bioreactor activities in function of
308 time. The hTMPK bioreactor was still active after 795 minutes, 21 uses and 60 days of
309 storage with a normalized remaining activity of 10%. The hNDPK bioreactor showed better
310 stability with a loss of 60% of the initial activity after 965 minutes, 20 uses and 68 days of
311 storage. The bioreactors can therefore be regenerated after each analysis and can be used for
312 multiple analyses performed over several days. Therefore, a limitation of this methodology
313 could turn out to be the decrease of bioreactor stability over the time. This limitation could be
314 easily overcome with the injection of a reference compound (such as dTMP).

315 **3.5. Application of the on-line methodology: study of ANPs specific conversion** 316 **regarding hTMPK and $\nu\nu$ TMPK**

317 ANPs have become a key class of antiviral nucleotide derivatives. Following their uptake,
318 ANPs undergo most often two phosphorylation steps catalyzed by cellular kinases to reach
319 their target, the viral DNA polymerase [11]. Concerning the ANPs study, the first
320 phosphorylation step (from MP to DP) is most often described as the rate-limiting step

321 (compared to DP-TP conversion) [10]. In this context, the developed on-line methodology
322 was applied to the study of the mono-phosphorylation step. The selectivity of antiviral therapy
323 is an important aspect in drug discovery and could have an important impact on
324 pharmacological and toxicological outcomes. One way to design site-selective therapy is the
325 use of viral kinases to convert pro-drug into active nucleoside triphosphate locally in the
326 infected cells. In this work, the feasibility of the on-line monitoring phosphorylation was
327 evaluated for the study of conversion specificity of two ANPs phosphorylations (Figure 1).
328 The ANPs containing a pyrimidine base were proven efficiently activated by viral and human
329 TMPK. The influence of the aliphatic chain length (3, 4 and 5 carbones) and the kind of C₅
330 substituent was evaluated. hTMPK was shown to efficiently phosphorylate (E)-isomer of
331 allylphosphonate uracil containing a methyl (ANP-CH₃) or a bromine (ANP-Br) at C₅-
332 position whereas v_vTMPK exhibited reduced activity towards both substrates [37]. hTMPK
333 and v_vTMPK activities regarding ANP-CH₃-MP and ANP-Br-MP were first evaluated by
334 UV-spectrophotometry assay and compared with activities toward the endogenous substrate
335 dTMP. Results are shown in supplementary data Table S1. hTMPK showed high activity
336 regarding the two ANPs with k_{cat}/K_M (ANP-CH₃-MP) = 25 000 M⁻¹ s⁻¹ and k_{cat}/K_M (ANP-Br-MP) = 9
337 000 M⁻¹ s⁻¹ (respectively 6 and 17 times lower than hTMPK activity regarding dTMP).
338 v_vTMPK showed lower activity regarding the same substrates with k_{cat}/K_M (ANP-CH₃-MP) = 1
339 380 M⁻¹ s⁻¹ and k_{cat}/K_M (ANP-Br-MP) = 1 200 M⁻¹ s⁻¹ (respectively 72 and 83 times lower than
340 v_vTMPK activity regarding dTMP).

341 The proof of concept was developed with the study of the endogenous compound dTMP
342 regarding two human kinase strains TMPK and NDPK. The study proved the feasibility of the
343 on-line method to directly monitor on-line phosphorylation. Two ANPs were then evaluated
344 to study the possible transposition of the method to other substrates (synthesized, with lower

345 conversion rate) regarding other kinase strains (*vaccina virus*), in order to show the potential
346 of the methodology to realize a screening of various compounds.

347 The feasibility of the on-line conversions was evaluated by direct infusion of dTMP, ANP-
348 CH₃-MP and ANP-Br-MP into immobilized hTMPK and *v*vTMPK bioreactors. As *v*vTMPK
349 shares similar structure with hTMPK [40] the two immobilization processes and efficiencies
350 were considered similar. The monitoring of the specific EIC of masses of interest offered a
351 direct monitoring of the reactions. *v*vTMPK activity was first validated by a
352 spectrophotometric assay. Results are shown in Table S1.

353 Figure 7 shows the EIC of interest during dTMP, ANP-CH₃-MP and ANP-Br-MP infusion
354 into active and denatured hTMPK bioreactor. Denatured hTMPK bioreactor gave no
355 conversion for the three substrates which attest to the absence of false positive. As expected
356 with our previous analysis, dTMP conversion was confirmed by infusion into active hTMPK
357 bioreactor. The on-line analyses of ANPs highlighted an accumulation of diphosphate form
358 after 15 min of infusion. Although the catalytic efficiencies of hTMPK regarding ANP-CH₃-
359 MP and ANP-Br-MP respectively were found lower than the catalytic efficiency of dTMP
360 conversion (Table S1), the on-line experiments and immobilized enzymes showed a good
361 correlation with a specific and significant conversion monitoring. Unlike natural substrate, the
362 diphosphate ANP standards are not commercially available. In addition, their ionization
363 disparity and the EIC intensity of diphosphate ANPs cannot be compared to evaluate reaction
364 efficiencies. Although, in this application, this approach is not quantitative, the latter offers
365 various attractive advantages such as a speed of analysis (4 min for dTMP and 15 min of
366 ANPs), a specificity of detection (without a chromatographic dimension), a versatility of
367 analysis (same analytical method for various synthetic compounds) and an identification of
368 the reaction product (HRMS detection) for a better knowledge of phosphorylation mechanism
369 of each drug. To confirm the effectiveness of this methodology, the same ANPs were

370 analyzed with the *vv*TMPK bioreactor. As shown in Figure 8, *vv*TMPK bioreactor activity
371 was first validated by dTMP infusion. The on-line experiments seem to be correlated with the
372 catalytic efficiency of free *vv*TMPK ($k_{cat}/K_{M(vvTMPK)} = 100\ 000\ \text{M}^{-1}\ \text{s}^{-1}$). Indeed, a significant
373 conversion of dTMP in dTDP was observed. In the case of *vv*TMPK, the dTMP conversion
374 was shown lower. In addition to a lower catalytic efficiency of *vv*TMPK, this lower
375 conversion is likely due to the storage time of the enzyme (hTMPK freshly produced).
376 In case of ANPs infusion into *vv*TMPK bioreactor, the results showed no conversion that
377 attest to the lack of false positive. These results are consistent with the results obtained with
378 the spectrophotometric test (Table S1). In order to improve the confidence of this
379 experiments, the off-line FIA-HRMS methodology was also performed to validate this
380 specificity of conversion. As shown in Figure S5, the on-line monitoring results are also
381 consistent with the off-line FIA-HRMS methodology. These two experiments showed the
382 feasibility of evaluating the activity specificity of the human and *vaccina virus* enzymatic
383 strains regarding two ANP compounds synthesized in the laboratory. These results validated the
384 absence of false positive and/or false negative thus validating the reliability of the on-line method.
385 Indeed, the results obtained with the FIA-HRMS method (off-line sample preparation, time-
386 consuming) with overnight reaction were shown similar to those obtained with the on-line
387 methodology within 15 minutes. This on-line methodology was proved reliable, rapid, automatable
388 and therefore suitable for a screening methodology.

389

390 **4. Conclusion**

391 This work shows for the first time the feasibility of an on-line MS methodology for the
392 conversion monitoring of nucleoside monophosphate (NMP) into nucleoside diphosphate
393 (NDP) and triphosphate (NTP). As a proof of concept, the two-phosphorylation steps from
394 thymidine monophosphate to thymidine triphosphate were monitored by the methodology.

395 This dynamic approach showed various attractive advantages such as specificity of detection,
396 speed of analysis (5 minutes), high conversion efficiency (> 50 %), substrate versatility (no
397 chromatographic dimension) and possible automation (for screening methodology). In this
398 context, this work offered an example of application of the on-line methodology for the
399 monitoring of conversion of two Acyclic Nucleoside phosphonates (ANPs) regarding human
400 and *vaccina virus* TMPK strains. This approach was proven reliable regarding the specificity
401 of conversion and results obtained were in agreement with the spectrophotometric and the
402 FIA-HRMS assays. Therefore, thanks to the longevity of bioreactor, the possible automation
403 and multi-step enzymatic monitoring, this methodology could be easily applied to the
404 metabolization study of various new potential antiviral drugs, whether for one step or for
405 multi-step phosphorylation

406 Although this work was developed by High-Resolution Mass Spectrometry, this methodology
407 is transposable to less expensive mass spectrometers (MRM mode). Actually, this
408 development can be applied to the study of other synthetic (pro)drugs in order to bring better
409 comprehension of a potential drug metabolic pathway: phosphorylation steps, specific activity
410 regarding human or viral enzymatic strains....

411

412 **ACKNOWLEDGMENTS:** LAA thanks Dr C El Amri and Dr D. Deville-Bonne of
413 University Pierre et Marie Curie (UPMC, Paris, France) for the generous gift of
414 nucleoside/nucleotide kinases and their plasmids. JF thanks the **Région Centre-Val de Loire**
415 for a PhD scholarship. We thank the LABEX SynOrg (ANR-11-LABX-0029) for partial
416 financial support.

417

418

419
420
421
422
423
424
425
426
427
428
429
430
431
432
433
434
435
436
437
438
439
440
441
442
443
444
445
446
447
448
449
450
451
452
453
454
455
456
457
458
459
460
461
462
463
464

[1] G.N. Kumar, S. Surapaneni, Role of drug metabolism in drug discovery and development, *Med Res Rev.* 5 (2001) 397-411.

[2] G. Apic, T. Ignjatovic, S. Boyer, R.B. Russel, Illuminating drug discovery with biological pathways, *Minireview* 579 (2005) 1872-1877.

[3] D. Topalis, R. Snoeck, G. Andrei, , Tenofovir activating kinases may impact the outcome of HIV treatment and prevention, *Ebiomedicine* 2 (2015) 1018-1019.

[4] T. Cihlar, A.S. Ray, Nucleoside and nucleotide HIV reverse transcriptase inhibitors: 25 years after zidovudine, *Antiviral Res.* 85(1) (2010) 39-58.

[5] J. Bourdais, R. Biondi, S. Sarfati, C. Guerreiro, L. Lascu, J. Janin, M. Véron, Cellular Phosphorylation of anti-HIV nucleosides, *J. Biol. Chem* 271(14) (1996) 7887-7890.

[6] E. De Clerq, Discovery and development of BVDU (brivudin) as a therapeutic for the treatment of herpes zoster, *Biochem Pharmacol* 68(12) (2004) 2301-15.

[7] E. De Clerq, A. Holy, Acyclic nucleoside phosphonates: a key class of antiviral drugs, *Nat. Rev. Drug Discov.* 4 (2005) 928-940.

[8] R.J. Whitley, Drug discovery for human immunodeficiency virus infection: conquests and hurdles, *J. Antimicrob. Chemother.* 37 (1996) 151-159.

[9] M. Baba, R. Pauwels, P. Herdewijn, E. De Clercq, J. Desmyter, M. Vandeputte, Both 2', 3'-dideoxythymidine and its 2', 3'-unsaturated derivative (2', 3'-dideoxythymidinene) are potent and selective inhibitors of human immunodeficiency virus replication in vitro, *Biochem. Biophys. Res. Commun* 142 (1987) 128-134.

[10] A. Lavie, M. Konrad, Structural requirements for efficient phosphorylation of nucleotide analogs by human thymidylate kinase, *J. Med. Chem.* 4 (2004) 351-359.

[11] D. Deville-Bonne, C. El Amri, P. Meyer, Y. Chen, L.A. Agrofoglio, J. Janin, Human and viral nucleoside/nucleotide kinases involved in antiviral drug activation: structural and catalytic properties, *Antiv. Res.* 86(1) (2010) 101-20.

[12] A.R. Van Rompay, M. Johansson, A. Karlsson, Substrate specificity and phosphorylation of antiviral and anticancer nucleoside analogues by human deoxyribonucleoside kinases and ribonucleoside kinases, *Pharmacol. Ther* 100(2) (2003) 119-139.

465 [13] E. De Clerq, Antiviral and antitumor activities of 5-substituted 2'-deoxyuridines., *Methods Find*
466 *Exp Clin Pharmacol.* 2 (1980) 253-267.

467 [14] Y. Zhang, Y. Gao, X. Wen, H. Ma, Current prodrug strategies for improving oral absorption of
468 nucleoside analogues, *AJPS* 9(2) (2014) 65-74.

469 [15] F. Pertusati, S. Serafini, N. Albadry, R. Snoeck, G. Andrei, Phosphonoamidate prodrugs of C5-
470 substituted pyrimidine acyclic nucleosides for antiviral therapy, *Antiv. Res.* 143 (2017) 262-268.

471 [16] A. Varga, E. Graczer, L. Chaloin, K. Liliom, P. Zavodszky, C. Lionne, M. Vas, Selectivity of kinases
472 on the activation of tenofovir, an anti-HIV agent, *Eur J Pharm Sci.* 48(1-2) (2013) 307-15.

473 [17] C. Blondin, L. Serina, L. Wiesmüller, A.M Gilles, O. Bârză, Improved spectrophotometric assay of
474 nucleoside monophosphate kinase activity using the pyruvate kinase/lactate dehydrogenase coupling
475 system, *Anal. Chem.* 220 (1994) 219-221.

476 [18] R.M. Lilley, D.A. Walker, An improved spectrophotometric assay for ribulosebiphosphate
477 carboxylase, *Biochim. Biophys. Acta* 358 (1974) 226-229.

478 [19] P. Schelling, G. Folkers, L. Scapozza, A spectrophotometric assay for quantitative determination
479 of *k_{cat}* of herpes simplex virus type 1 thymidine kinase substrates, *Anal. Biochem.* 295(1) (2001) 82-
480 7.

481 [20] B. N. Stretcher, A. J. Pesce, P. T. Frame, D. S. Stein, Pharmacokinetics of Zidovudine
482 Phosphorylation in Peripheral Blood Mononuclear Cells from Patients Infected with Human
483 Immunodeficiency Virus, *Antimicrob. Agents Chemother.*, 38 (1994) 1541-1547.

484 [21] R. R. Drake, T. N. Wilbert, T. A. Hinds, K. M. Gilbert, Differential ganciclovir-mediated cell killing
485 by glutamine 125 mutants of herpes simplex virus type 1 thymidine kinase, *J. Biol. Chem.* 274 (1999)
486 37186-37192.

487 [22] I. G. Giles, P. C. Poat, K. A. Munday, The kinetics of rabbit muscle pyruvate kinase, *Biochem. J.*
488 157 (1976) 577-589.

489 [23] M. Faria, M.S. Halquist, E. Kindt, W. Li, H.T. Karnes, P.J. O'Brien, Liquid chromatography-tandem
490 mass spectrometry method for quantification of thymidine kinase activity in human serum by
491 monitoring the conversion of 3'-deoxy-3'-fluorothymidine to 3'-deoxy-3'-fluorothymidine
492 monophosphate, *J Chromatogr B Analyt Technol Biomed Life Sci* 907 (2012) 13-20.

493 [24] C.C. Liu, J.S. Huang, D.L. Tyrrell, N.J. Dovichi, Capillary electrophoresis-electrospray-mass
494 spectrometry of nucleosides and nucleotides: application to phosphorylation studies of anti-human
495 immunodeficiency virus nucleosides in a human hepatoma cell line, *Electrophoresis* 26(7-8) (2005)
496 1424-31.

497 [25] Y. Qi, Y. Li, J.J. Bao, Development of a capillary electrophoresis method for analyzing adenosine
498 deaminase and purine nucleoside phosphorylase and its application in inhibitor screening, *Anal.*
499 *Biochem.* 506 (2016) 31-44.

500 [26] H.F. Tzeng, H.P. Hung, Simultaneous determination of thymidylate and thymidine diphosphate
501 by capillary electrophoresis as a rapid monitoring tool for thymidine kinase and thymidylate kinase
502 activities, *Electrophoresis* 26(11) (2005) 2225-30.

503 [27] L. Zhu, L. Chen, H. Luo, X. Xu, Frontal Affinity Chromatography Combined On-Line with Mass
504 Spectrometry: A Tool for the Binding Study of Different Epidermal Growth Factor Receptor
505 Inhibitors, *Anal. Chem.* 75 (2003) 6388-6393.

506 [28] E. Calleri, C. Temporini, G. Massolini, Frontal affinity chromatography in characterizing
507 immobilized receptors, *J. Pharm. Biomed. Anal* 54(5) (2011) 911-925.

508 [29] E. Calleri, C. Temporini, B. Caccianlanza, G. Massolini, Target-Based Drug Discovery: the
509 Emerging Success of Frontal Affinity Chromatography Coupled to Mass Spectrometry,
510 *ChemMedChem* 4 (2009) 905-916.

511 [30] X. Song, J. Cui, J. Li, H. Yan, L. Li, L. Wen, Y. Geng, D. Wang, A novel bioreactor for highly efficient
512 biotransformation of resveratrol from polydatin with high-speed counter-current chromatography,
513 *LWT* 103 (2019) 192-198.

514 [31] J. Guo, H. Lin, J. Wang, Y. Lin, T. Zhang, Z. Jiang, Recent advances in bio-affinity chromatography
515 for screening bioactive compounds from natural products, *J Pharm Biomed Anal* 165 (2019) 182-197.

- 516 [32] T. Slechtova, M. Gilar, K. Kalikova, S.M. Moore, J.W. Jorgenson, E. Tesarova, Performance
517 comparison of three trypsin columns used in liquid chromatography, *J. Chrom. A* 1490 (2017) 126-
518 132.
- 519 [33] K.I. Kasai, Y. Oda, M. Nishikata, S.I. Ishii, Frontal affinity chromatography: Theory for its
520 application to studies on specific interactions of biomolecules, *J. Chrom. B Biomed Sci Appl* 376
521 (1986) 33-47.
- 522 [34] H.C. Foo, N.W. Smith, S.M. Stanley, Fabrication of an on-line enzyme micro-reactor coupled to
523 liquid chromatography-tandem mass spectrometry for the digestion of recombinant human
524 erythropoietin, *Talanta* 135 (2015) 18-22.
- 525 [35] S. Bhattacharya, M. Schiavone, J. Gomes, S.K. Bhattacharya, Cascade of bioreactors in series for
526 conversion of 3-phospho-D-glycerate into D-ribulose-1,5-bisphosphate: kinetic parameters of
527 enzymes and operation variables, *J. Biotechnol.* 111(2) (2004) 203-17.
- 528 [36] J. Yin, T. Xu, N. Zhang, H. Wang, Three-Enzyme Cascade Bioreactor for Rapid Digestion of
529 Genomic DNA into Single Nucleosides, *Anal. Chem.* 88(15) (2016) 7730-7.
- 530 [37] D. Topalis, U. Pradere, V. Roy, C. Caillat, A. Azzouzi, J. Broggi, R. Snoeck, G. Andrei, J. Lin, S.
531 Eriksson, J.A. Alexandre, C. El-Amri, D. Deville-Bonne, P. Meyer, J. Balzarini, L.A. Agrofoglio, Novel
532 antiviral C5-substituted pyrimidine acyclic nucleoside phosphonates selected as human thymidylate
533 kinase substrates, *J Med Chem* 54(1) (2011) 222-32.
- 534 [38] S. Pochet, L. Dugue, G. Labesse, M. Delepierre, H. Munier-Lehmann, Comparative study of purine
535 and pyrimidine nucleoside analogues acting on the thymidylate kinases of *Mycobacterium*
536 *tuberculosis* and of humans, *Chembiochem* 4(8) (2003) 742-7.
- 537 [39] J. Ferey, D. Da Silva, C. Colas, R. Nehmé, P. Lafite, V. Roy, P. Morin, R. Daniellou, L. Agrofoglio, B.
538 Maunit, Monitoring of successive phosphorylations of thymidine using free and immobilized human
539 nucleoside/nucleotide kinases by Flow Injection Analysis with High-Resolution Mass Spectrometry,
540 *Anal. Chim. Acta* (2018).
- 541 [40] C. Caillat, D. Topalis, L.A. Agrofoglio, S. Pochet, J. Balzarini, D. Deville-Bonne, P. Meyer, Crystal
542 structure of poxvirus thymidylate kinase: an unexpected dimerization has implications for antiviral
543 therapy, *Proc Natl Acad Sci USA* 105(44) (2008) 16900-5.

544

545

546

547

548

549

550

551

552

553

554

555

556
557
558
559
560
561
562
563
564
565
566
567
568
569
570
571
572
573
574
575
576
577
578
579
580
581
582

Figure captions

Figure 1: Chemical formula of (a) Acyclic Nucleoside Phosphonate-CH₃ (ANP-CH₃-MP) and (b) Acyclic Nucleoside Phosphonate-Br (ANP-Br-MP).

Figure 2: On-line experiment methodology; 2 sample loops of 320 μL connected to the two bioreactors in series via a 10-port valve. The bioreactors are directly connected to the high-resolution mass spectrometer via an electrospray source. The autosampler injects a solution “1” in the loop 1 (position valve 1-2) with the loading pump. The valve switches to position 1-10 to infuse solution “1” into the bioreactors with the analytical pump. During solution “1” infusion, a solution “2” is loaded into the loop 2 with the loading pump (position valve 1-10). When the infusion is completed (time infusion programmed in the method), the valve switches to position 1-2 and loop 2 is infused with the analytical pump.

583 **Figure 3:** hTMPK bioreactor; monitoring of EIC for dTMP and dTDP (m/z 321.0500 [M-H]⁻ for
584 dTMP, m/z 401.0166 [M-H]⁻ for dTDP) for (a) denatured and (b) active bioreactors. [dTMP] = 20 μM
585 ([ATP] = 150 μM, [MgCl₂] = 200 μM), flow rate = 60 μL min⁻¹, mobile phase: ammonium acetate
586 buffer (50 mM, pH = 7). Valve switch every 3 minutes.

587

588 **Figure 4:** hNDPK bioreactor; monitoring of EIC for dTDP and dTTP (m/z 401.0166 [M-H]⁻ for dTDP
589 and m/z 480.9831 [M-H]⁻ for dTTP) for (a) denatured and (b) active bioreactors. [dTDP] = 20 μM
590 ([ATP] = 150 μM, [MgCl₂] = 200 μM), flow rate = 40 μL min⁻¹, mobile phase: ammonium acetate
591 buffer (50 mM, pH = 7). Valve switch: 5 minutes.

592

593 **Figure 5:** enzymatic cascade; monitoring of EIC for dTMP, dTDP and dTTP (m/z 321.0500 [M-H]⁻
594 for dTMP, m/z 401.0166 [M-H]⁻ for dTDP and m/z 480.9831 [M-H]⁻ for dTTP) for (a) denatured and
595 (b) active bioreactors. [dTMP] = 20 μM ([ATP] = 150 μM, [MgCl₂] = 200 μM), flow rate = 40 μL
596 min⁻¹, mobile phase: ammonium acetate buffer (50 mM, pH = 7). Valve switch: 5 minutes.

597 **Figure 6:** stability of bioreactors. Conversion efficiency: hTMPK was used 21 times (795 minutes,
598 37°C) over 60 days (diamonds) and hNDPK was used 20 times (915 minutes, 37°C) over 68 days
599 (squares).

600

601 **Figure 7:** Active and denatured hTMPK bioreactor; monitoring of EIC for dTMP (m/z 321.0500),
602 ANP-CH₃-MP (m/z 259.0562) and ANP-Br-MP (m/z 322.0561) conversion into dTMP (m/z
603 401.0166), ANP-CH₃-DP (m/z 339.0150) and ANP-Br-DP (m/z 402.0149). Solution of 20 μM of each
604 substrate ([MgCl₂] = 200 μM, [ATP] = 150 μM, 50 mM AcNH₄, pH = 7). Flow rate = 60 μL min⁻¹.

605

606 **Figure 8:** Active vTMPK bioreactor; monitoring of EIC for dTMP (m/z 321.0500), ANP-CH₃-MP
607 (m/z 259.0562) and ANP-Br-MP (m/z 322.0561) conversion into dTMP (m/z 401.0166), ANP-CH₃-
608 DP (m/z 339.0150) and ANP-Br-DP (m/z 402.0149). Solution of 20 μM of each substrate ([MgCl₂] =
609 200 μM, [ATP] = 150 μM, 50 mM AcNH₄, pH = 7). Flow rate = 60 μL min⁻¹.

610

611

612 **Table captions**

613

614 **Table 1:** m/z values of Thymidine Monophosphate (dTMP), Thymidine Diphosphate (dTDP),
615 Thymidine Triphosphate (dTTP), methyl allylphosphonate uracil (ANP-CH₃) and bromine
616 allylphosphonate uracil (ANP-Br).

617

618

619

620

621

622

623

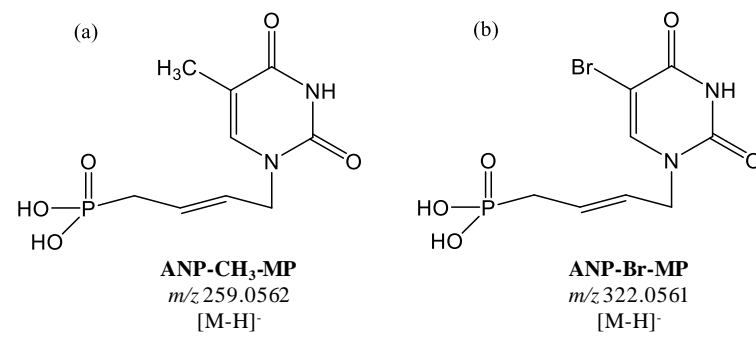


Figure 1: Chemical formula of (a) Acyclic Nucleoside Phosphonate-CH₃ (ANP-CH₃-MP) and (b) Acyclic Nucleoside Phosphonate-Br (ANP-Br-MP).

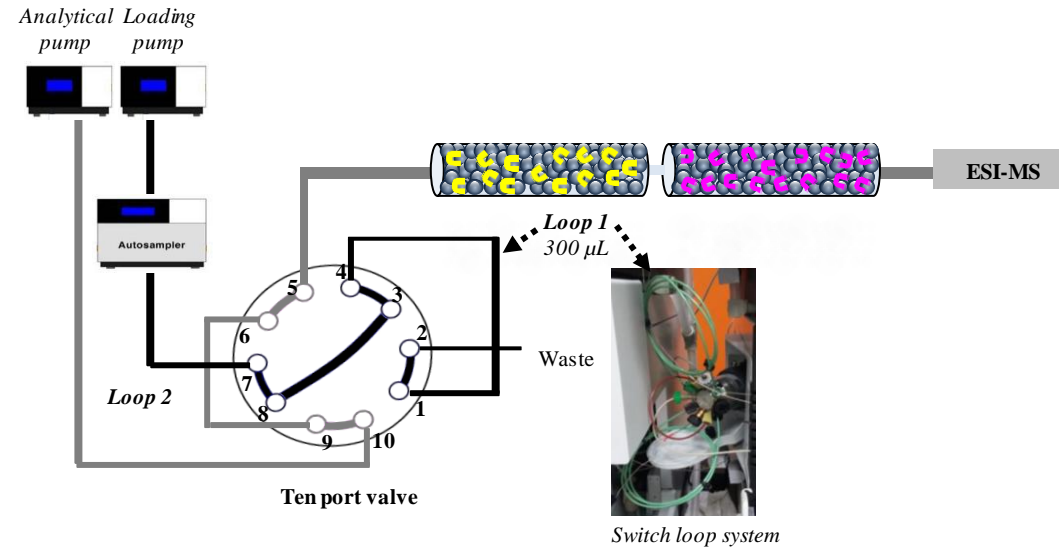


Figure 2: On-line experiment methodology; 2 sample loops of 320 µL connected to the two bioreactors in series via a 10-port valve. The bioreactors are directly connected to the high-resolution mass spectrometer via an electrospray source. The autosampler injects a solution "1" into the loop 1 (position valve 1-2) with the loading pump. The valve switches to position 1-10 to infuse solution "1" into the bioreactors with the analytical pump. During solution "1" infusion, a solution "2" is loaded into the loop 2 with the loading pump (position valve 1-10). When the infusion is completed (time infusion programmed in the method), the valve switches to position 1-2 and loop 2 is infused with the analytical pump.

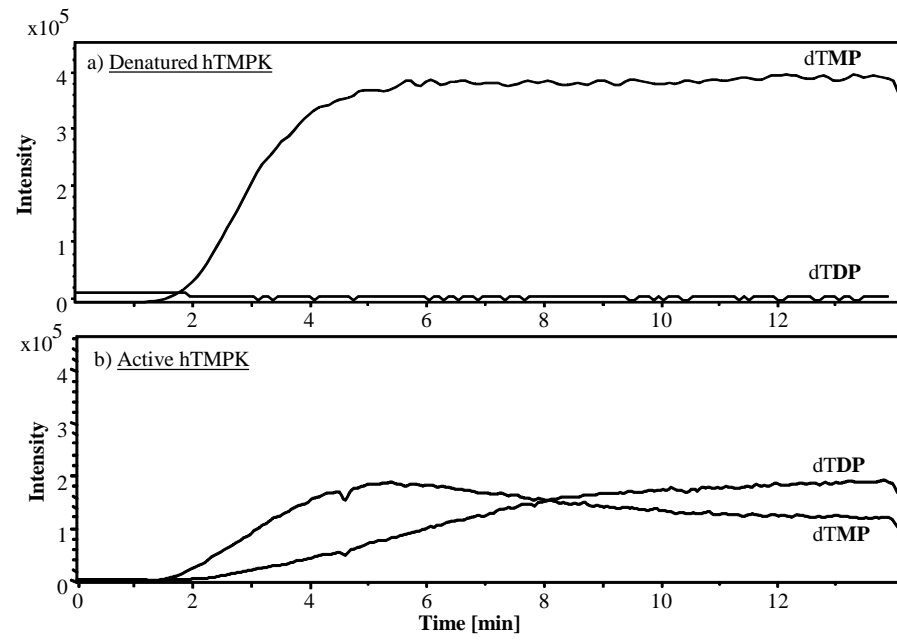


Figure 3: hTMPK bioreactor; monitoring of EIC for dTMP and dTDP (m/z 321.0500 [M-H]⁻ for dTMP, m/z 401.0166 [M-H]⁻ for dTDP) for (a) denatured and (b) active bioreactors. [dTMP] = 20 μ M ([ATP] = 150 μ M, [MgCl₂] = 200 μ M), flow rate = 60 μ L min⁻¹, mobile phase: ammonium acetate buffer (50 mM, pH = 7). Valve switch every 3 minutes.

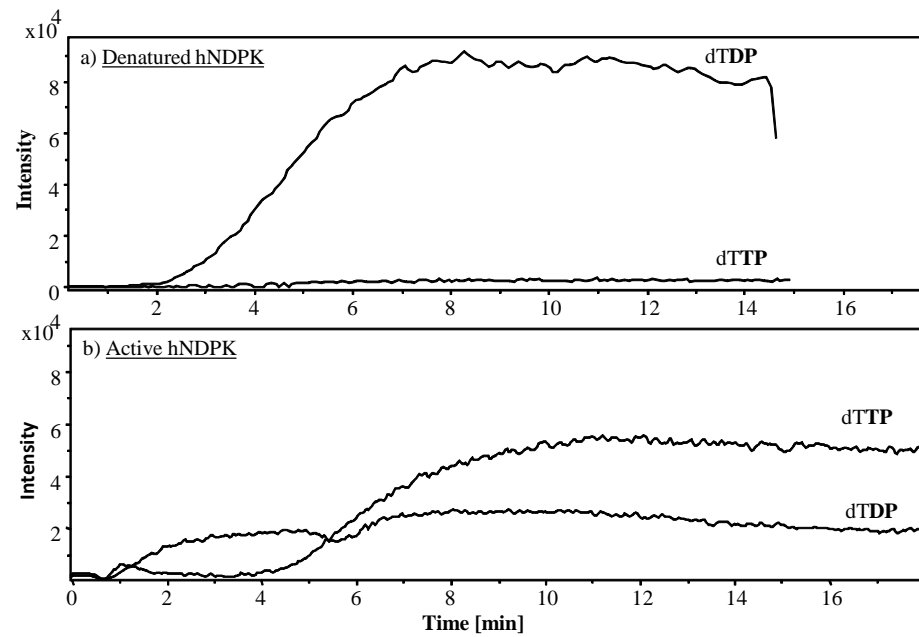


Figure 4: hNDPK bioreactor; monitoring of EIC for dTDP and dTTP (m/z 401.0166 [M-H]⁻ for dTDP and m/z 480.9831 [M-H]⁻ for dTTP) for (a) denatured and (b) active hNDPK. [dTDP] = 20 μ M ([ATP] = 150 μ M, [MgCl₂] = 200 μ M), flow rate = 40 μ L min⁻¹, mobile phase: ammonium acetate buffer (50 mM, pH = 7). Valve switch: 5 minutes.

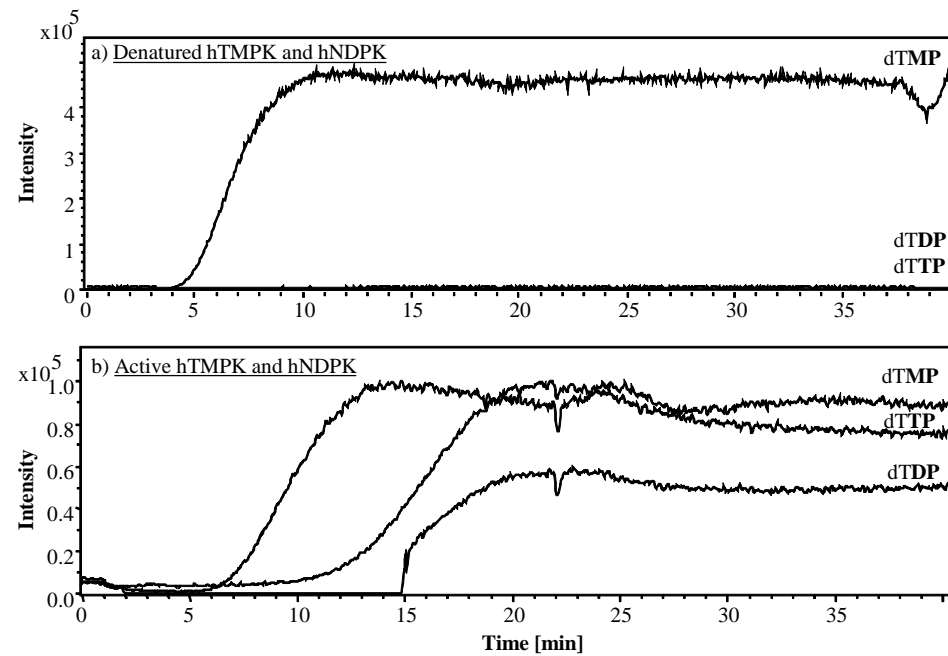


Figure 5: enzymatic cascade; monitoring of EIC for dTMP, dTDP and dTTP (m/z 321.0500 [M-H]⁻ for dTMP, m/z 401.0166 [M-H]⁻ for dTDP and m/z 480.9831 [M-H]⁻ for dTTP) for (a) denatured and (b) active bioreactors. [dTMP] = 20 μ M ([ATP] = 150 μ M, [MgCl₂] = 200 μ M), flow rate = 40 μ L min⁻¹, mobile phase: ammonium acetate buffer (50 mM, pH = 7). Valve switch: 5 minutes.

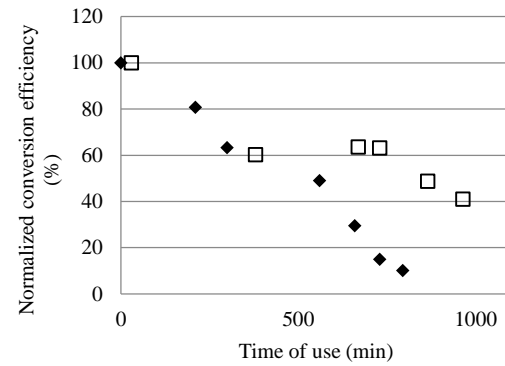


Figure 6: stability of bioreactors. Conversion efficiency: hTMPK was used 21 times (795 minutes, 37°C) over 60 days (diamonds) and hNDPK was used 20 times (915 minutes, 37°C) over 68 days (squares).

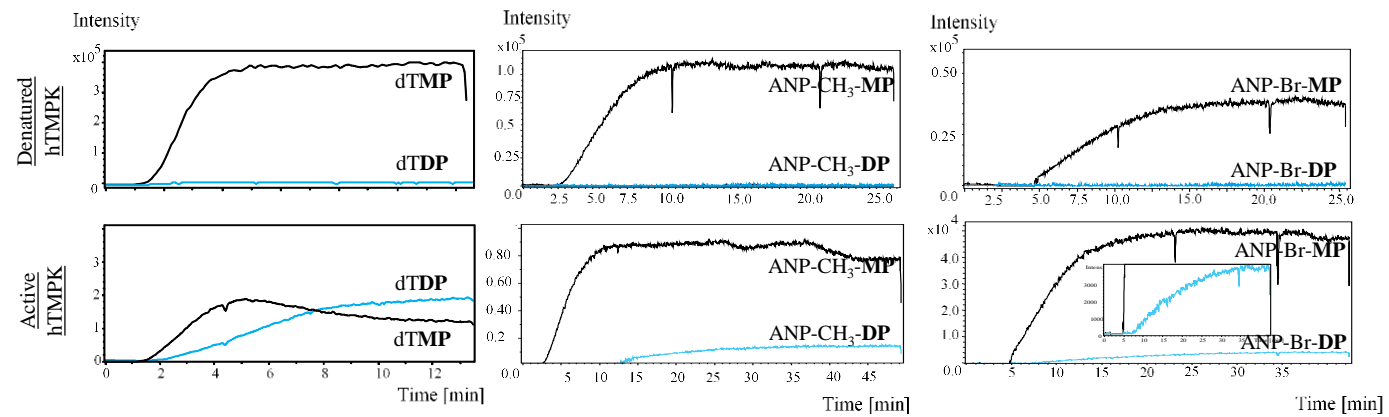


Figure 7: Active and denatured hTMPK bioreactor; monitoring of EIC for dTMP (m/z 321.0500), ANP-CH₃-MP (m/z 259.0562) and ANP-Br-MP (m/z 322.0561) conversion into dTDP (m/z 401.0166), ANP-CH₃-DP (m/z 339.0150) and ANP-Br-DP (m/z 402.0149). Solution of 20 μ M of each substrate ([MgCl₂] = 200 μ M, [ATP] = 150 μ M, 50 mM AcNH₄, pH = 7). Flow rate = 60 μ L min⁻¹.

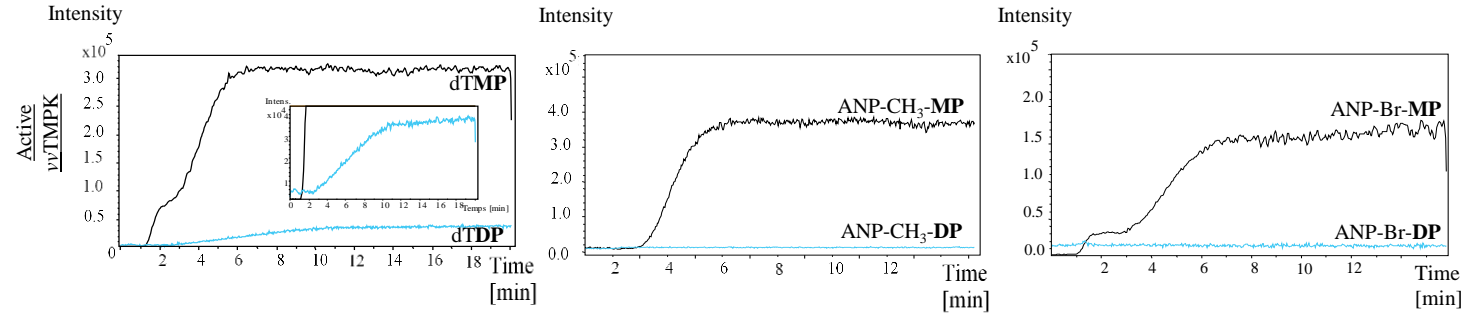


Figure 8: Active vvtMPK bioreactor; monitoring of EIC for dTMP (m/z 321.0500), ANP-CH₃-MP (m/z 259.0562) and ANP-Br-MP (m/z 322.0561) conversion into dTMP (m/z 401.0166), ANP-CH₃-DP (m/z 339.0150) and ANP-Br-DP (m/z 402.0149). Solution of 20 μ M of each substrate ($[MgCl_2] = 200 \mu$ M, $[ATP] = 150 \mu$ M, 50 mM AcNH₄, pH = 7). Flow rate = 60 μ L min⁻¹.

Endogenous				
$[M-H]^-$	dTMP	dTDP	dTTP	
m/z	321.0500	401.0166	480.9831	
ANPs				
$[M-H]^-$	ANP-CH ₃ -MP	ANP-CH ₃ -DP	ANP-Br-MP	ANP-Br-DP
m/z	259.0562	339.0150	322.0561	402.0149

Table 1: m/z values of Thymidine Monophosphate (dTMP), Thymidine Diphosphate (dTDP), Thymidine Triphosphate (dTTP), methyl allylphosphonate uracil (ANP-CH₃) and bromine allylphosphonate uracil (ANP-Br).

